JOURNAL OF PROPULSION AND POWER
Vol. 14, No. 5, September–October 1998

Advanced Rocket Nozzles

Gerald Hagemann*
DLR, German Aerospace Research Center, Lampoldshausen 74239, Germany
Hans Immich†
Daimler–Benz AG, Munich 81663, Germany
Thong Van Nguyen‡
GenCorp Aerojet, Sacramento, California 95813
and
Gennady E. Dumnov§
Keldysh Research Center, Moscow 125438, Russia

Several nozzle concepts that promise a gain in performance over existing conventional nozzles are discussed in this paper. It is shown that significant performance gains result from the adaptation of the exhaust flow to the ambient pressure. Special attention is then given to altitude-adaptive nozzle concepts, which have recently received new interest in the space industry. Current research results are presented for dual-bell nozzles and other nozzles with devices for forced flow separation and for plug nozzles with external freestream expansion. In addition, results of former research on nozzles of dual-mode engines such as dual-throat and dual-expander engines and on expansion–deflection nozzles are shown. In general, flow adaptation induces shocks and expansion waves, which result in exit profiles that are quite different from idealized one-dimensional assumptions. Flow phenomena observed in experiments and numerical simulations during different nozzle operations are highlighted, critical design aspects and operation conditions are discussed, and performance characteristics of selected nozzles are presented. The consideration of derived performance characteristics in launcher and trajectory optimization calculations reveal significant payload gains at least for some of these advanced nozzle concepts.

Nomenclature

A = area
F = thrust
h = flight altitude
I = impulse
l = length
$\dot{m}$ = mass flow rate
p = pressure
$\bar{r}$ = mass ratio oxidizer/fuel mixture
r = radius
x, y = coordinates
ε = nozzle area ratio

Subscripts
amb = ambient
c = combustion chamber
cr = critical
e = exit plane
geom = geometrical
ref = reference
sp = specific
t = throat
vac = vacuum
w = wall

Received Sept. 2, 1997; revision received Feb. 27, 1998; accepted for publication March 19, 1998.

*Research Engineer, Ph.D., Space Propulsion. E-mail: gerald.hagemann@dlr.de.
†Research Engineer, Ph.D., Space Infrastructure. E-mail: Im24344@dbmail.dase.de. Member AIAA.
‡Technical Principal, Ph.D. E-mail: thong.nguyen@aerojet.com. Member AIAA.
§Division Head, Ph.D., Aerothermodynamics. E-mail: dumnov@relay.rinet.ru.

I. Introduction

THE reduction of Earth-to-orbit launch costs in conjunction with an increase in launcher reliability and operational efficiency are the key demands on future space transportation systems, like single-stage-to-orbit vehicles (SSTO). The realization of these vehicles strongly depends on the performance of the engines, which should deliver high performance with low system complexity.

Performance data for rocket engines are practically always lower than the theoretically attainable values because of imperfections in the mixing, combustion, and expansion of the propellants. Figure 1 illustrates the different loss sources in rocket engine nozzles. The examination and evaluation of these loss effects is and has for some time been the subject of research at scientific institutes and in industry. Table 1 summarizes performance losses in the thrust chambers and nozzles of typical high-performance rocket engines: The SSME- and Vulcain 1 engine[1] (Space Shuttle main engine, Rocketdyne hydrogen–oxygen engine and hydrogen–oxygen core engine of European Ariane-5 launcher). Among the important loss sources in thrust chambers and nozzles are viscous effects because of turbulent boundary layers and the nonuniformity of the flow in the exit area, whereas chemical nonequilibrium effects can be neglected in H_2–O_2 rocket engines with chamber pressures above $p_c = 50$ bar.[1] Furthermore, the nonadaptation of the exhaust flow to varying ambient pressures induces a significant negative thrust contribution (see Figs. 2–4). Ambient pressures that are higher than nozzle wall exit pressures also increase the danger of flow separation inside the nozzle, resulting in the possible generation of side loads. A brief description of state-of-the-art prediction methods for both phenomena is given.

Table 1 Performance losses in conventional rocket nozzles[a]

Losses	Vulcain 1, %	SSME, %
Chemical nonequilibrium	0.2	0.1
Friction	1.1	0.6
Divergence, nonuniformity of exit flow	1.2	1.0
Imperfections in mixing and combustion	1.0	0.5
Nonadapted nozzle flow	0–15	0–15

[a]Other loss sources also shown in Fig. 1.

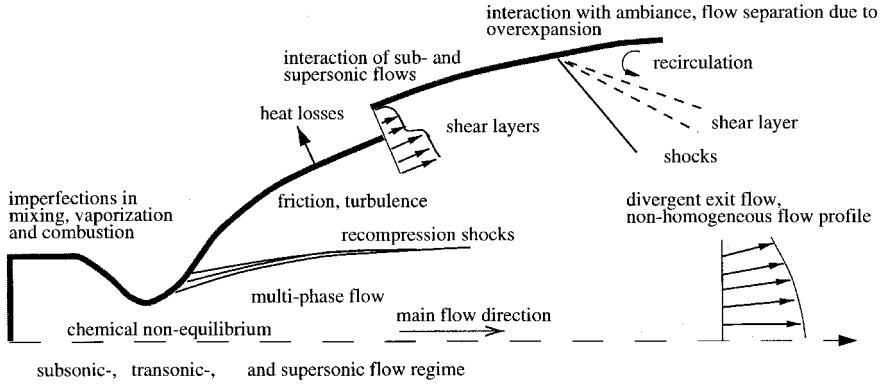

Fig. 1 Flow phenomena and loss sources in rocket nozzles.

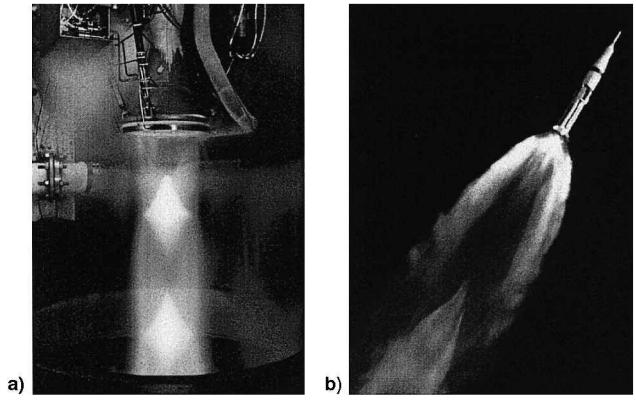

Fig. 2 Rocket nozzle flowfields during off-design operation: a) overexpanded flow RL10A-5 engine and b) underexpanded flow Saturn-1B, Apollo-7 (Photographs, United Technologies Pratt & Whitney, NASA).

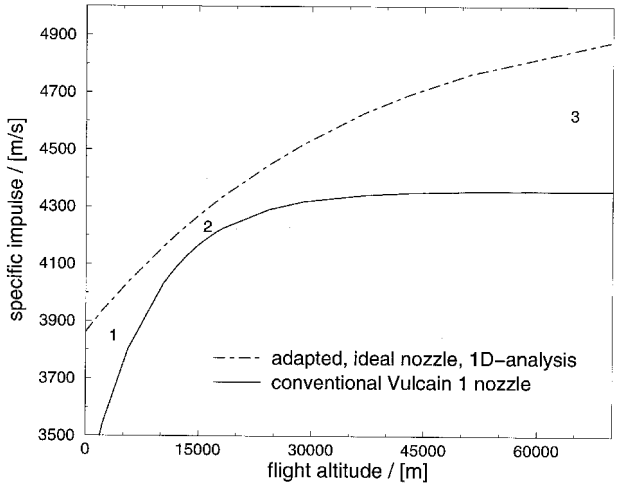

Fig. 3 Performance data for nozzle of Vulcain 1 engine (design parameters of Vulcain 1 nozzle: $\varepsilon = 45$, $p_c/p_{amb} = 555$, $\bar{r} = 5.89$).

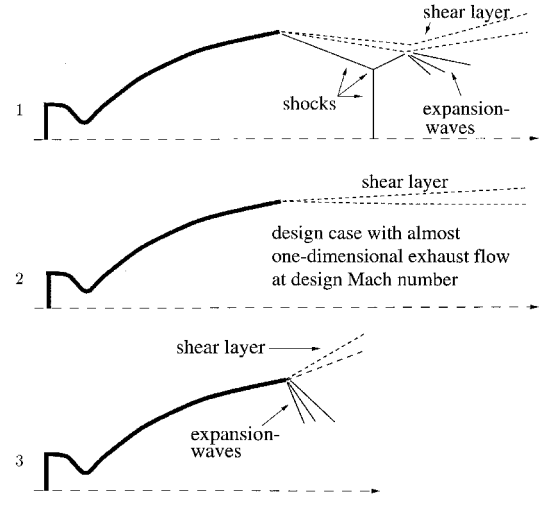

Fig. 4 Flow phenomena for a conventional rocket nozzle.

The main part of the paper addresses different nozzle concepts with improvements in performance as compared to conventional nozzles achieved by altitude adaptation and, thus, by minimizing losses caused by over- or underexpansion. Several concepts for the altitude adaptation of rocket nozzles exist in the literature and these are considered in this paper in more detail.[2–4] This discussion of advanced nozzles includes nozzles with inserts for controlled flow separation, two-position nozzles, dual-bell nozzles, dual-expander and dual-throat nozzles, expansion–deflection nozzles, and plug nozzles. In the past, practically all of these concepts have been the subject of analytical and experimental work.[5–7] Although benefits in performance were indicated in most of the available publications, none of these nozzle concepts has yet been used in existing rocket launchers. This may change in the near future, because a rocket engine with a linear plug nozzle is foreseen as the propulsion system for the Lockheed Martin lifting body RLV X-33 concept.

II. Conventional Nozzles

Conventional bell-type rocket nozzles, which are in use in practically all of today's rockets, limit the overall engine per-

formance during the ascent of the launcher owing to their fixed geometry. Significant performance losses are induced during the off-design operation of the nozzles, when the flow is overexpanded during low-altitude operation with ambient pressures higher than the nozzle exit pressure, or underexpanded during high-altitude operation with ambient pressures lower than the nozzle exit pressure. Figure 2 shows photographs of nozzle exhaust flows during off-design operation. In the case of overexpanded flow, oblique shocks emanating into the flowfield adapt the exhaust flow to the ambient pressure. Further downstream, a system of shocks and expansion waves leads to the characteristic barrel-like form of the exhaust flow. In contrast, the underexpansion of the flow results in a further expansion of the exhaust gases behind the rocket.

Off-design operations with either overexpanded or underexpanded exhaust flow induce performance losses. Figure 3 shows calculated performance data for the Vulcain 1 nozzle as function of ambient pressure, together with performance data for an ideally adapted nozzle. Flow phenomena at different pressure ratios p_c/p_{amb} are included in Fig. 4. [The sketch with flow phenomena for the lower pressure ratio p_c/p_{amb} shows a normal shock (Mach disk). Depending on the pressure ratio, this normal shock might not appear, see, e.g., Fig. 2.] The Vulcain 1 nozzle is designed in such a manner that no uncontrolled flow separation should occur during steady-state operation at low altitude, resulting in a wall exit pressure of $p_{w,e} \approx 0.4$ bar, which is in accordance with the Summerfield criterion.[8] The nozzle flow is adapted at an ambient pressure of $p_{amb} \approx 0.18$ bar, which corresponds to a flight altitude of $h \approx 15{,}000$ m, and performance losses observed at this ambient pressure are caused by internal loss effects (friction, divergence, mixing), as shown in Fig. 1 and Table 1. Losses in performance during off-design operations with over- or underexpansion of the exhaust flow rise up to 15%. In principle, the nozzle could be designed for a much higher area ratio to achieve better vacuum performance, but the flow would then separate inside the nozzle during low-altitude operation with an undesired generation of side-loads.

A. Flow Separation and Side-Loads

Flow separation in overexpanding nozzles and its theoretical prediction have been the subject of several studies in the past,[3,4,8] and different physical models and hypotheses for the prediction of flow separation have been developed. In strongly overexpanding nozzles, the flow separates from the wall at a certain pressure ratio of wall pressure to ambient pressure, p_w/p_{amb}. The typical structure of the flowfield near the separation point is shown in Fig. 5, together with wall pressure data. Separation and the formation of a recirculation zone at the wall induce an oblique shock wave near the wall, which leads to a recompression of the flow.

The physical phenomenon of flow separation can be divided into two simple phenomena.[3] The first is the turbulent boundary-layer separation from the nozzle wall, which is characterized by the ratio of the nozzle wall pressure just after the separation, p_p, to the nozzle wall pressure just before separation, p_{sep}. This pressure ratio is referred to as the critical pressure ratio $p_{cr} = p_{sep}/p_p = p_1/p_2$. The second phenomenon is connected with the flow in the separated zone, which is characterized by a minor pressure gradient along the wall. The analysis of model experimental data on separated turbulent supersonic flows shows that the pressure ratio p_{cr} is equal for separated flows before an obstacle, and for separated nozzle flows.[3] For turbulent flows p_{cr} shows a slight dependence on Reynolds number, but depends strongly on Mach number. Furthermore, investigations of separated flows in rocket engine nozzles showed that p_{cr} is also a function of wall temperature, gas composition, and nozzle wall roughness.

Various approaches to the prediction of flow separation are used in industry and research institutes. For example, the Keldysh Center's method for the determination of the flow separation point in rocket nozzles is based on empirical relationships obtained for p_{cr}, $p_p/p_{w,e}$, and $p_{w,e}/p_{amb}$. Using these relations, the pressure ratio p_{sep}/p_{amb}, the separation point, and the wall pressure distribution are determined. Aerojet uses tabulated data for the prediction of flow separation from various experiments with conical and bell-shaped nozzles.[4] At a known pressure ratio of chamber pressure to ambient pressure, a lower and an upper separation pressure ratio follows from the database that is different for conical and bell-shaped nozzles. A separation criterion used at the European industry and scientific institutes describes the pressure ratio p_{sep}/p_{amb} as function of the local flow Mach number at the wall near the separation point. This analytical model was derived from various cold- and hot-firing tests of overexpanding nozzles.[9]

Various numerical simulations of flow problems featuring flow separation have shown that the numerical prediction of flow separation with state-of-the-art turbulence modeling results in good agreement with experimental data.[3,10] As an example, Figs. 6 and 7 compare experimental and numerical data on wall pressure ratios in two overexpanding nozzles. Furthermore, former experiments of separated flows indicated that there is a random movement of the separation line in overexpanding rocket nozzles,[9,11,12] resulting in the possible generation of side loads. The correct prediction of side-loads with models is uncertain, and still a subject of on-going research. Common side-load models described in Refs. 4 and 9 assume that the separation line in the nozzle has a maximum tilt angle

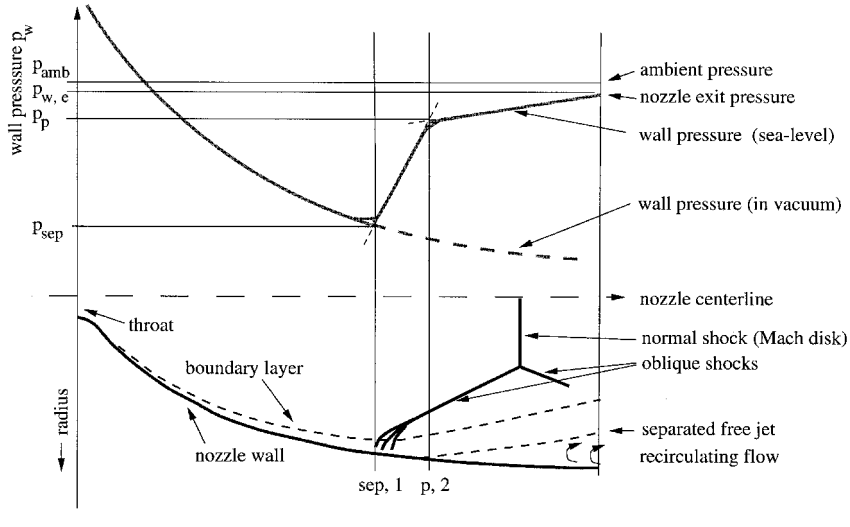

Fig. 5 Flow separation in overexpanding rocket nozzles, wall pressure profile, and phenomenology.

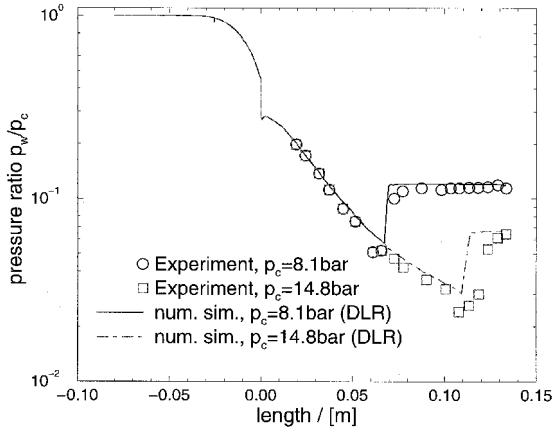

Fig. 6 Experimental and numerical data on wall pressure ratios in overexpanding conical nozzles with flow separation. Cold-gas test case with subscale conical nozzle.

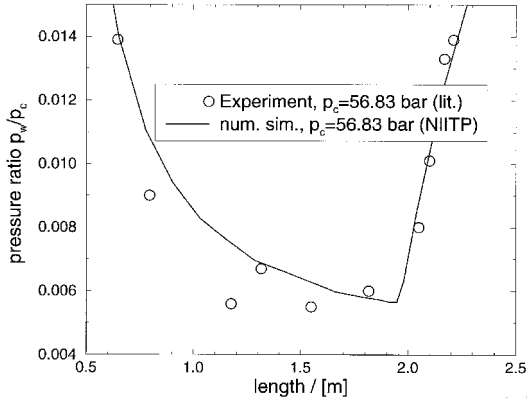

Fig. 7 Experimental and numerical data on wall pressure ratios in overexpanding bell nozzles with flow separation. Hot-gas test case with J-2S engine.

with the centerline. The minimum and maximum separation points are predicted using the upper and lower separation data that result from the applied separation model. In the case of distinct separation points as obtained with the Summerfield- or Schmucker-criterion, a certain scattering around the predicted separation point is assumed. The side-load is then calculated by integrating the wall pressure in the asymmetrical flow separation region.[4,9] These approaches gave reasonable results for the J2-S and Vulcain 1 nozzle.

At the Keldysh Center in Russia, model experiments of separated flow effects on side-loads acting on nozzles began in the early 1980s.[11] These investigations were directed mainly to the determination of the unsteady pressure fluctuations in the separation zone on the whole engine. The method is described in Ref. 11 in more detail, it is based on a generalization of obtained empirical data for the spectral density of the pulsating pressure field in the separation zone. Distribution of the pressure amplitudes is governed by probability density functions. This method was validated with the experimental rms-values of side-loads acting on the RD-0120 nozzle (CABD hydrogen–oxygen engine, first-stage engine of Russian Energia launcher). Other hypotheses for the appearance and prediction of side-loads also exist, e.g., based on aeroelastic analyses,[13] which account for the coupling of flow oscillations with thin nozzle shells. However, these hypotheses require experimental verification and validation.

Side-loads are an undesired phenomenon that may result in the destruction of the rocket nozzle and should therefore be avoided. In Ref. 9, the destruction of a J-2D engine (Rocketdyne hydrogen–oxygen engine, second- and third-stage engine of Saturn-5 launcher) as a result of side-loads is reported. The transient startup of the rocket engine generates a nozzle flow with uncontrolled flow separation and with possible side-load generation in the nozzle, whereas maximum area ratios of all first-stage nozzles or booster nozzles are chosen to avoid flow separation at the nominal chamber pressure operation. As a result, the vacuum performance of rocket engines that operate during the entire launcher trajectory, such as the SSME or Vulcain 1 engines, is limited.

B. Potential Performance Improvements

Compared to existing rocket engines, a gain in performance is achieved with advanced engines such as mixed-mode propulsion systems, dual-mixture ratio engines, or dual-expander engines. Nevertheless, the upgrade of existing engines with better performing subsystems, such as turbines and pumps, also leads to a gain in overall performance data and is discussed in more detail in Ref. 14. Nozzle performance of conventional rocket engines is already very high with regard to internal loss effects (friction, nonuniformity). However, for nozzles of gas-generator open-cycle engines such as the Vulcain 1 engine, a slight improvement in performance can be achieved with turbine exhaust gas (TEG) injection into the main nozzle as realized in the F-1 (kerosene–oxygen engine, first stage of Saturn-5 launcher) and J-2S, and it is foreseen for the Vulcain 2 engine (hydrogen–oxygen engine, upgrade of Vulcain 1 engine), and confirmed by numerical simulations[13,15,16] and experimental results.[3] This is mainly achieved through lower friction losses in the main nozzle[13,15] and because the bypass nozzles used for the expansion of the TEGs, which have higher divergence losses, are removed.

Despite the slight performance gain by TEG injection, the low-pressure near-wall stream of the injected gas favors a reduction of the critical pressure ratio at which flow separation occurs and, therefore, an earlier nozzle flow separation.[3,12] Furthermore, the presence of the secondary exhaust gas injection complicates nozzle-contouring methods with regard to the avoidance of uncontrolled flow separation for first-stage or booster nozzles.

III. Altitude Adaptive Nozzles

A critical comparison of performance losses shown in Table 1 reveals that most significant improvements in nozzle performance for first-stage or SSTO engines can be achieved through the adaptation of nozzle exit pressures to the variations in ambient pressure during the launcher's ascent through the atmosphere. Various concepts have been previously mentioned and will be discussed in detail in the following text.

A. Nozzles with Devices for Controlled Flow Separation

Several nozzle concepts with devices for controlled flow separation have been proposed in the literature, with primary emphasis on the reduction of side-loads during sea level or low-altitude operation. But the application of these concepts also results in an improved performance through the avoidance of significant overexpansion of the exhaust flow.

1. Dual-Bell Nozzle

This nozzle concept was first studied at the Jet Propulsion Laboratory[17] in 1949. In the late 1960s, Rocketdyne patented this nozzle concept, which has received attention in recent years in the U.S. and Europe.[6,7,18,19] Figure 8 illustrates the design of this nozzle concept with its typical inner base nozzle, the wall inflection, and the outer nozzle extension. This nozzle concept offers an altitude adaptation achieved only by nozzle wall inflection. In low altitudes, controlled and symmetrical flow separation occurs at this wall inflection (Fig. 9), which results in a lower effective area ratio. For higher altitudes, the nozzle flow is attached to the wall until the exit plane, and the full geometrical area ratio is used. Because of the higher area ratio, an improved vacuum performance is achieved. However, additional performance losses are induced in dual-bell nozzles,

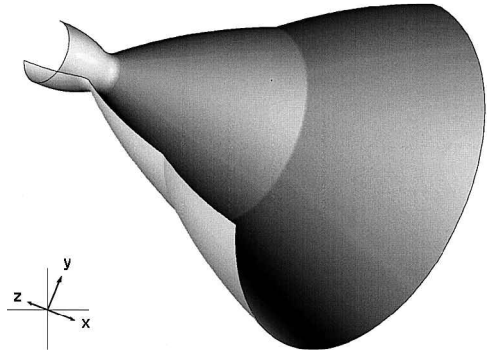

Fig. 8 Sketch of a dual-bell nozzle.

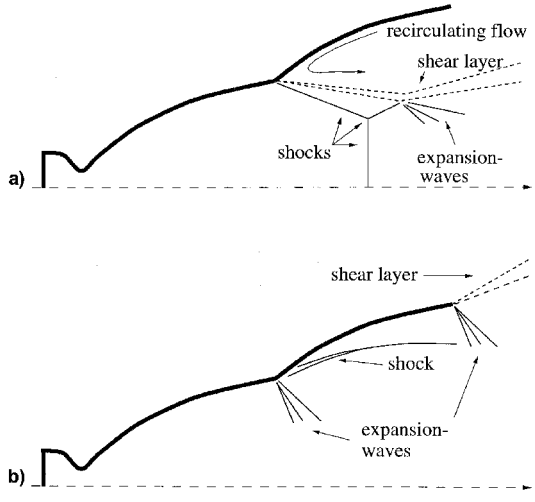

Fig. 9 Flowfield phenomena in dual-bell nozzles: a) sea-level mode with flow separation at the wall inflection point and b) altitude mode with a full-flowing nozzle.

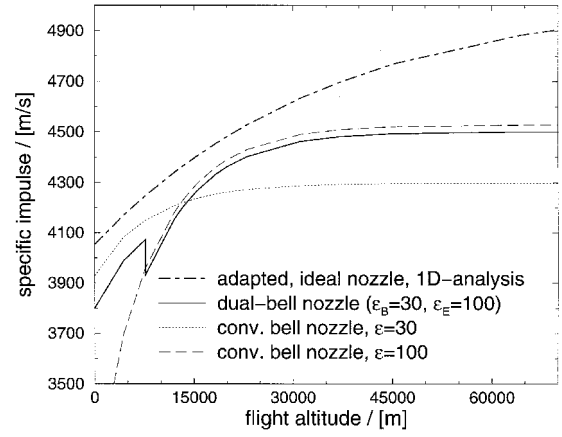

Fig. 10 Performance data of a dual-bell nozzle. Performance is compared with two baseline bell-type nozzles as function of flight altitude (baseline nozzle 1: same area ratio as dual-bell base nozzle; baseline nozzle 2: same area ratio as nozzle extension).

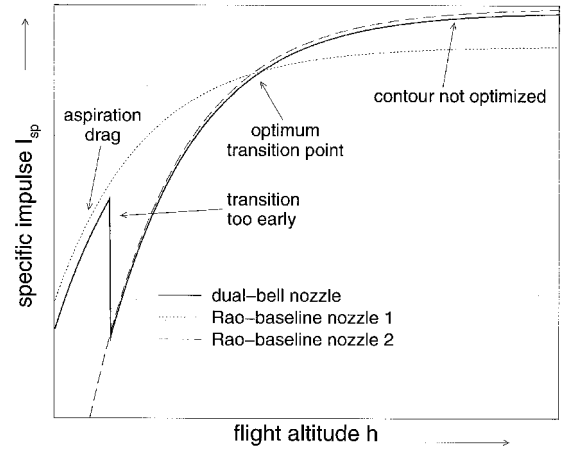

Fig. 11 Performance characteristics of a dual-bell nozzle. Performance is compared with two baseline bell-type nozzles as function of flight altitude (baseline nozzle 1: same area ratio as dual-bell base nozzle; baseline nozzle 2: same area ratio as nozzle extension).

as compared with two baseline nozzles having the same area ratio as the dual-bell nozzle at its wall inflection and in its exit plane. Figures 10 and 11 illustrate the performance of a dual-bell nozzle as a function of flight altitude in comparison with both baseline bell-type nozzles. (Design parameters of the dual-bell nozzle are taken from a launcher analysis published in Ref. 18: Propellants hydrogen/oxygen, $\bar{r} = 6$, $p_c = 200$ bar, $r_t = 0.07$ m, wall inflection at area ratio $\varepsilon_B = 30$, and total area ratio $\varepsilon_E = 100$.) The pressure within the separated flow region of the dual-bell nozzle extension at sea-level operation is slightly below the ambient pressure, inducing a thrust loss referred to as "aspiration drag." In addition, flow transition occurs before the optimum crossover point, which leads to further thrust loss as compared to an ideal switchover. The nonoptimum contour of the full flowing dual-bell nozzle results in further losses at high altitudes.

To gain insight into the performance and flow behavior of dual-bell nozzles at different ambient pressures, extensive numerical simulations with parametrical variations of contour design parameters were performed.[18] An optimized bell nozzle with equal total length and area ratio was used as the reference nozzle for comparison. As a result the vacuum performance of the dual-bell nozzles has a degradation because of the imperfect contour, and this additional loss has the same order of magnitude as the divergence loss of the optimized bell nozzle.

The simulations of sea-level operation also revealed an additional performance loss because of aspiration drag, which is less than 3% for these dual-bell nozzles. This additional loss depends linearly on the ambient pressure and, therefore, it is reduced during the ascent of the launcher. Furthermore, these simulations showed that the application of commonly used separation criteria derived for conventional nozzles and applied to dual-bell nozzles with their wall inflection to estimate the critical pressure ratio yields reasonable results with an accuracy of ≈15%. Experimental data obtained at the Keldysh Center revealed that the critical pressure ratio at the wall inflection is about 15–20% less than the critical pressure ratio of a conventional nozzle, and that usual separation criteria must be corrected for an accurate prediction of the critical wall pressure ratio.

Flow transition behavior in dual-bell nozzles strongly depends on the contour type of the nozzle extension.[3,6,18] A sudden transition from sea-level to vacuum operation can be, at least theoretically, achieved by two different extensions, with a zero wall pressure gradient (constant pressure extension), or a positive wall pressure gradient (overturned extension). But a critical analysis of the transition behavior considering decreasing ambient pressures during the launcher ascent revealed that a considerable time with uncontrolled flow separation within the nozzle extension exists even for these types of extensions. The duration of this period can be reduced drastically by throttling the chamber pressure.[18]

The main advantage of dual-bell nozzles as compared to other means of controlling nozzle flow separation is its simplicity because of the absence of any movable parts and, therefore, its high reliability. It is necessary to note that the external flow over the vehicle in flight reduces the pressure in the vehicle base region, where engines are installed. The ambient

pressure triggering the flow transition is the vehicle base pressure instead of the atmospheric pressure at the specific flight altitude. As the base pressure is lower than the atmospheric pressure, the nozzle flow transition occurs at a lower altitude than the one showed in Fig. 11, which slightly decreases the efficiency of the dual-bell nozzle operation along the trajectory.

Despite the additional losses induced in dual-bell nozzles, they still provide a significant net impulse gain over the entire trajectory as compared to conventional bell nozzles. Independent combined launcher and trajectory analyses performed by Dasa within the European Space Agency Future European Space Transportation Investigations Program (ESA FESTIP) study[19] and at DLR on SSTO vehicles powered with dual-bell nozzles result in a significant payload gain when compared with a reference launcher equipped with conventional nozzles.

2. *Nozzles with Fixed Inserts*

A trip ring attached to the inside of a conventional nozzle disturbs the turbulent boundary layer and causes flow separation at higher ambient pressures. At higher altitudes with lower ambient pressures the flow reattaches to the wall behind the trip ring, and full flowing of the nozzle is achieved. The transition from sea level to vacuum mode depends on the wall pressure near the trip-ring location and on the disturbance induced by the trip ring. The size of the trip ring is a compromise between stable flow separation during sea-level operation and the induced performance loss during vacuum operation. In Ref. 9 it is reported that a trip-ring size of 10% of the local boundary-layer thickness is sufficient to ensure stable flow separation.

In principle, this concept is similar to the dual-bell nozzle concept with regard to performance characteristics, as shown in Fig. 11 The sea-level performance of this nozzle concept is lower than the performance of a conventional bell nozzle truncated at the trip-ring location, because of the aspiration drag in the separated flow region of the nozzle. Furthermore, at sea level the bell nozzle with trip rings has even higher divergence losses than a comparable dual-bell nozzle, because the nozzle contour upstream of the obstacle differs from the optimal contour for this low-area ratio, as a result of the bell nozzle design for best vacuum performance. The additional losses induced during vacuum operation is about 1%, compared with the performance of the bell nozzle without an obstacle. Thus, the additional losses are comparable to the additional losses induced in dual-bell nozzles. As for dual-bell nozzles, the transition behavior of this nozzle concept is uncertain, but it will be even more uncertain than for a dual-bell nozzle with a constant pressure or overturned nozzle extension.

In principle, several altitude adaptations can be achieved with one nozzle by various trip rings, mounted one behind the other. However, this results in increasing vacuum performance losses. The trip rings can also be attached into existing nozzles and, therefore, represent a low-cost concept, at least for test purposes, with low technological risk. Trip rings have been demonstrated to be effective for side-load reductions during the transient startup of rocket engines.[20] The main problems with trip-ring nozzles are not only performance losses, but also ring resistance in high-temperature boundary layers, the exact circumferential fixing, and the uncertainties in the transition behavior. These uncertainties might be why active interest in this nozzle concept in the 1970s, which is documented in various publications,[9,20–22] has disappeared in recent years.

A further concept with a fixed wall discontinuity is a nozzle with a circumferential groove. The aerodynamic behavior of a nozzle with a groove and nozzle with trip rings are quite similar,[9] but this concept is hard to realize in the case of thin nozzle shells, which are used in all of today's rocket nozzles.

3. *Nozzles with Temporary Inserts*

Nozzle concepts with fixed wall discontinuities have the disadvantage of lower vacuum performance as compared with a conventional bell nozzle with equal design and operation data. A promising concept for controlled flow separation is therefore temporary inserts, which are removed for vacuum operation. These inserts can be either ablative or ejectible. The inserts may have the form of a complete secondary nozzle[23] (Fig. 12), or of small steps attached inside the nozzle wall. In case of ejectible inserts, a reliable mechanism is needed to provide a sudden and symmetrical detachment. In any case, shocks are induced during the transient ejection because the inserts act as an obstacle in the supersonic exhaust flow. These shocks also interact with the nozzle walls and increase pressure loads on the wall and local heat fluxes. A nonsymmetrical ejection would then result in the generation of side-loads. Furthermore, the danger of a downstream collision with the nozzle wall arises because the inserts might also experience a transversal movement toward the walls.

Recent hot-firing tests performed in Russia with a modified RD-0120 engine, equipped with a secondary nozzle insert, revealed a significant performance gain of 12% during the sea-level operation at 100% chamber pressure, compared with the original RD-0120 performance.[23] Nominal chamber pressure of this engine is p_c = 206 bar, with an area ratio of ε = 85.7. These full-scale, hot-firing tests demonstrated the durability of materials, sealings, and the release mechanism and, thus, the feasibility of this concept. Figure 12 shows the nozzle hardware and a sketch of the secondary nozzle mounted inside the RD-0120 nozzle.[23]

The principle performance characteristics of this RD-0120 nozzle with ejectible insert are included in Fig. 13. The nozzle operation with insert results in a slight performance loss compared with an ideal bell nozzle with the same reduced area

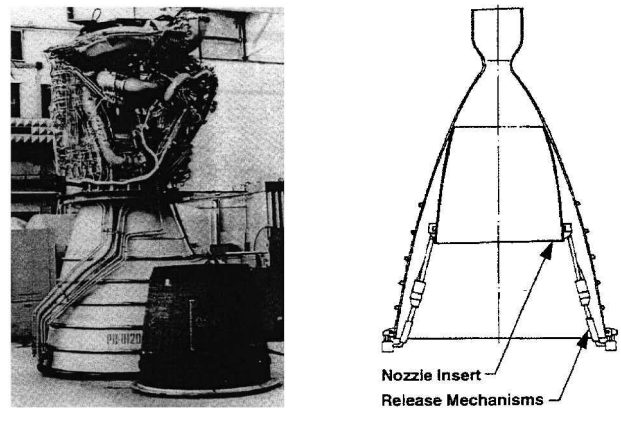

Fig. 12 RD-0120 nozzle hardware with removed nozzle insert and sketch of secondary nozzle mounted inside of the RD-0120 nozzle (photographs taken from Ref. 23).

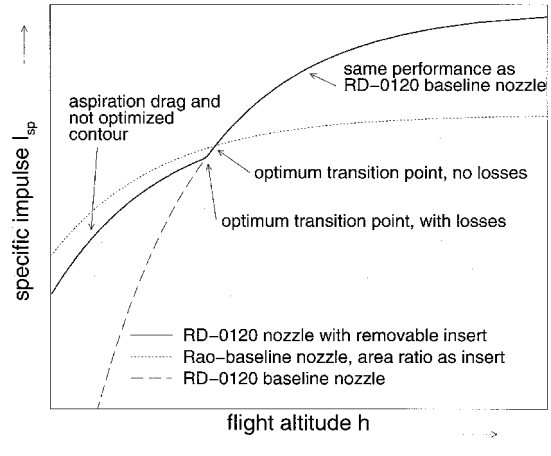

Fig. 13 Principle performance characteristics of the nozzle with insert.

ratio, because of aspiration drag and the presumably nonoptimized insert contour. The performance degradation is comparable to the one induced in dual-bell nozzles during sea-level operation (Fig. 11). In vacuum or high-altitude operations, the higher performance of the baseline nozzle is achieved.

Another method for removing the inserts is to use combustible or ablative elements.[9,24] During the ascent of the launcher the size of the insert is continuously reduced until it is completely consumed, resulting in a full flowing bell nozzle with a clean contour for best vacuum performance. The principal uncertainties of this nozzle concept are the stability and surface regression rates of the inserts. Furthermore, a homogeneous, symmetrical, and temporally defined consumption must be guaranteed, despite possible local pressure and temperature fluctuations near the nozzle walls. This is currently highly uncertain.

4. Nozzles with Active or Passive Secondary Gas Injection

With this nozzle concept the flow in an overexpanding nozzle is forced to separate at a desired location by injecting a second fluid into the gas stream in the wall normal direction, to achieve maximum disturbance of the main exhaust gas and, thus, to induce flow separation. This secondary gas injection is quite different from the aforementioned TEG injection, which should be injected with few or no disturbances to the main flow. The injection could be either active, that is, forced through gas expansion from a higher-pressure reservoir, or passive, using holes in the wall through which ambient gas is sucked in (vented nozzle concept). The latter concept can only work in case of gas pressures near the wall inside the nozzle that are lower than the ambient pressure. Experience on forced secondary gas injection gained at Aerojet shows that a large amount of injected fluid is required to induce a significant flow separation. Furthermore, no net specific impulse gain is realized when considering the additional gas flow rate.

In the vented nozzle concept segments of the bell nozzle wall have various slots or holes opened to the outside ambient pressure. During low-altitude operation the slots are opened to trigger flow separation within the nozzle, whereas the slots are closed during high-altitude or vacuum operation, so that the gas fully expands inside the entire nozzle. Experiments with a modified RL10A-3 engine, equipped with this nozzle concept, were performed at Pratt & Whitney.[25] Performance results showed that over a small range of low-pressure ratios the perforated nozzle performed as well as a nozzle with its area ratio truncated immediately upstream of the vented area. However, at above some intermediate pressure ratios, the thrust efficiency suddenly dropped and approached that of the full-flowing nozzle. The measured performance characteristics were quite similar to those of the dual-bell nozzles shown in Fig. 11.

The altitude range of this nozzle concept is limited by the number and position of the holes because the pressure within the nozzle must be lower than the ambient pressure. Furthermore, as the rocket aft-body base pressure is lower than the altitude atmospheric pressure in the surrounding ambient flows, the nozzle flow transition occurs at a lower altitude and, thus, the range of compensation is further reduced.

5. Two-Position or Extendible Nozzles

Nozzles of this type with extendible exit cones are currently used only for rocket motors of upper stages to reduce the package volume for the nozzle, e.g., at present for solid rocket engines such as the inertial upper stage (IUS), or for the liquid rocket engine RL10. The main idea of the extendible extension is to use a truncated nozzle with low expansion in low-flight altitudes and to have a higher nozzle extension at high altitudes. Figure 14 illustrates this nozzle concept. Its capability for altitude compensation is indisputable and the nozzle performance is easily predictable. The whole nozzle contour including the extendible extension is contoured for maximum

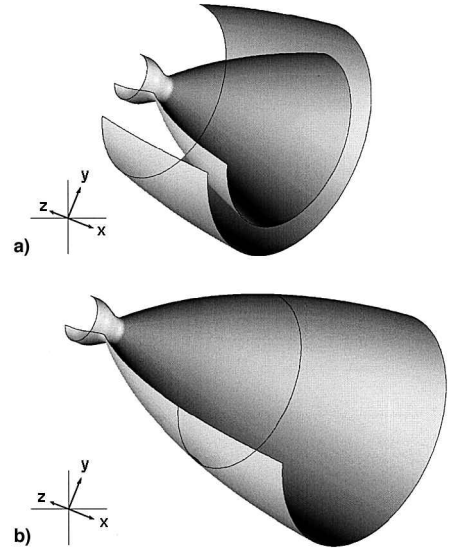

Fig. 14 Sketch of a two-position nozzle during a) sea-level and b) vacuum operations.

performance at the high-area ratio with either the method of characteristics or a variational method. The area ratio of the first nozzle section is then determined and the nozzle contour is divided into two parts: The fixed nozzle part and the extendible extension. Investigations conducted at the Keldysh Center have shown that this nozzle-contouring method is not only the simplest but also provides a good overall trajectory performance.[3] A minor performance loss is incorporated during low-altitude operations because of the truncated inner nozzle, which has a nonoptimal contour for this interim exit area ratio. The performance characteristics as a function of flight altitude are similar to those of the nozzle with the ejectible insert, as shown in Fig. 13. A tradeoff study performed at the Keldysh Center on nozzles with an ejectible insert and an extendible extension showed that the thrust characteristics of the nozzle with an ejectible insert are slightly better than those of the extendible nozzle concept, with the same overall dimensions for both nozzles.

The main drawback of the extendible nozzle concept is that it requires mechanical devices for the deployment of the extension, which reduces engine reliability and increases total engine mass. The necessity for active cooling of the extendible extension requires flexible or movable elements in the cooling system, which also reduces system reliability. The influences of the external flow and the generated jet noise on the extendible extension in the retracted, initial position, have not yet been fully investigated. Former investigations conducted in the Keldysh Center showed that the external flow causes both steady and unsteady pressure loads on the retracted nozzle extension, whereas the engine jet noise causes strong vibrations of the nozzle extension.

B. Plug Nozzles

Various experimental, analytical, and numerical research on plug nozzles have been performed since the 1950s in the U.S.,[4,5,32–35] Europe,[5,7,10,19,26,27], Russia,[3] and Japan.[28] In contrast to the previously discussed nozzle concepts, plug nozzles provide, at least theoretically, a continuous altitude adaptation up to their geometrical area ratio. Figures 15 and 16 show two different design approaches for circular plug nozzles, which differ only in the chamber and primary nozzle layout. A conical central body is shown here, which could also be designed with more sophisticated contouring methods.[29,30] Different design approaches include plug nozzles with a toroidal chamber and throat (with and without truncation) and plug nozzles with a cluster of circular bell nozzle modules or with clustered quasirectangular nozzle modules. The latter approach seems to

be advantageous because further losses induced by the gaps between individual modules and the flowfield interactions downstream of the module exits can be minimized. It has been shown that transition from a round to a square nozzle results in a very small performance loss.[31] In principle, the flowfield development of a clustered plug nozzle with rectangular nozzle modules is similar to that of a toroidal plug nozzle, but avoids the inherent disadvantages of the toroidal plug design regarding 1) the control of a constant throat gap during manufacturing and thermal expansion (side-loads and thrust vector deviations); 2) the cooling of toroidal throat with tiny throat gaps; and 3) the control of combustion instabilities in the toroidal combustion chamber. Another plug nozzle configuration is the linear plug nozzle, which is foreseen for the propulsion system of the RLV X-33 concept.

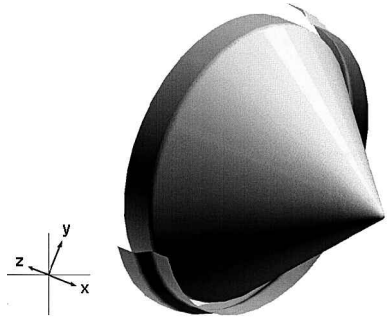

Fig. 15 Principle design of plug nozzles, toroidal plug, full length.

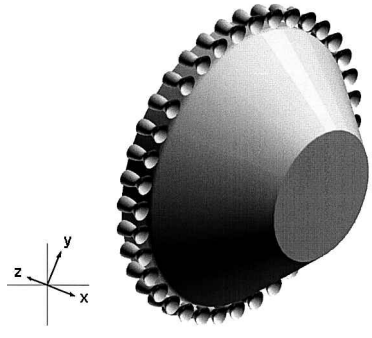

Fig. 16 Principle design of plug nozzles, clustered plug, 36 modules, with truncated plug body.

1. *Circular Plug Nozzles*

Figure 17 summarizes the principle flow phenomena of circular plug nozzles with full length and truncated central bodies at different off-design (top and bottom) and design (center) pressure ratios that were observed in experiments and numerical simulations. For pressure ratios lower than the design pressure ratio of a plug nozzle with a well-contoured central body, the flow expands near the central plug body without separation, and a system of recompression shocks and expansion waves adapts the exhaust flow to the ambient pressure p_{amb}. The characteristic barrel-like form with several inflections of the shear-layer results from various interactions of compression and expansion waves with the shear layer, and turbulent diffusion enlarges the shear layer farther downstream of the throat. The existence of the overexpansion and recompression processes is inferred from up- and down-variations of plug wall pressure profiles observed in various cold-flow tests and numerical simulations, and will also be shown later for linear plug nozzles.

At the design pressure ratio (see Fig. 17, left column, center), the characteristic with the design Mach number should be a straight line emanating to the tip of the central plug body, and the shear layer is parallel to the centerline. However, for circular plug nozzles designed with contouring methods proposed in Refs. 29 and 30, no exact one-dimensional exit flow profile can be achieved, because both methods use the Prandtl–Meyer relations that are only valid for planar flows. Furthermore, nonhomogeneous flow in the throat region, which is in general not considered within the contour design process, also influences the exit flow profile. The wall pressure distribution remains constant at pressure ratios above the design pressure ratio, i.e., the plug nozzle behaves like a conventional nozzle, the loss of its capability of further altitude

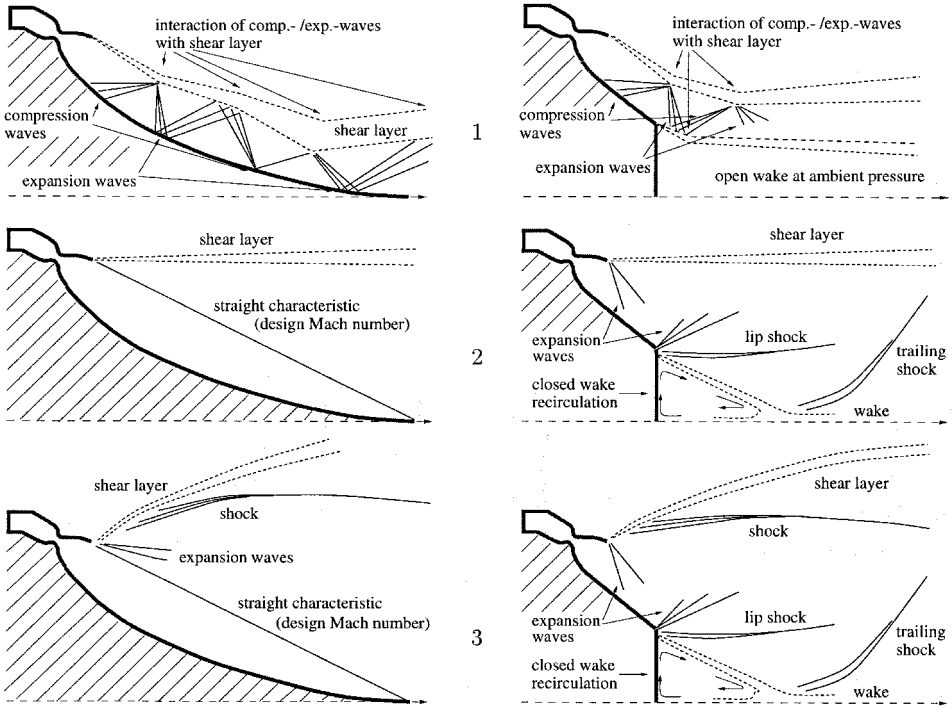

Fig. 17 Flow phenomena of a plug nozzle with full length (left column) and truncated central body (right column) at different pressure ratios p_c/p_{amb}, off-design (top, bottom) and design (center) pressure ratio.

Table 2 Design parameters of toroidal plug nozzles

Design data	Full-scale nozzle[a]	Subscale nozzle[b]
Chamber pressure p_c	100 bar	12 bar
Propellants	Hydrogen/oxygen	Gas–oil/nitric-acid
Mixture ratio $\bar{r}$	6.0	2.5
Inner chamber diameter $d_{c,\text{inner}}$	4.3 m	0.19 m
Outer chamber diameter $d_{c,\text{outer}}$	4.4 m	0.34 m
Geometric area ratio ε	55	10

[a]Used for numerical simulations and performance predictions, see Fig. 18.
[b]Used in experiments, see Fig. 20.

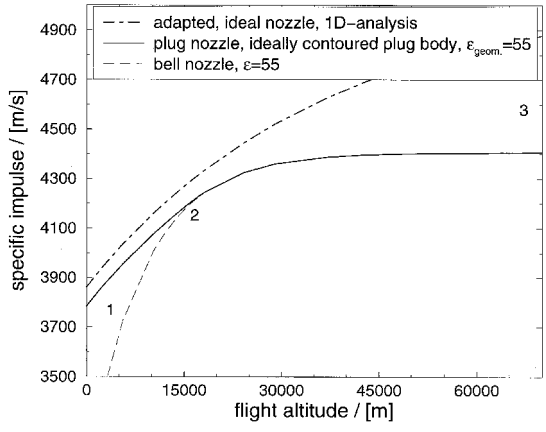

Fig. 18 Performance of numerically simulated plug nozzle with full-length central body.

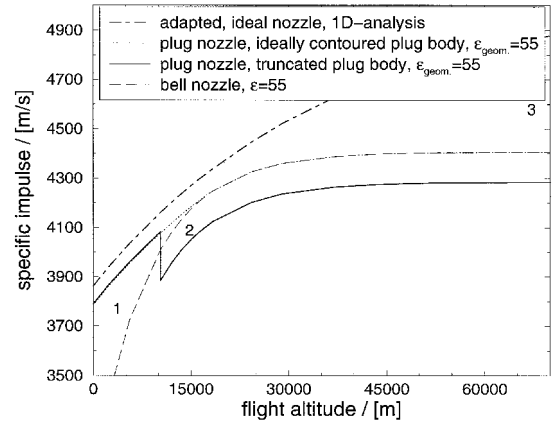

Fig. 19 Performance of numerically simulated plug nozzle with truncated central body.

adaptation being included. Figure 17 (left column, bottom) illustrates the flowfield at higher pressure ratios. Performance data of a typical plug nozzle are included in Fig. 18 and compared to a conventional bell nozzle with equal area ratio. The design and combustion chamber parameters are included in the left column of Table 2.[27]

The truncation of the central plug body, which is an advantage because of the huge length and high structural mass of the well-contoured central body, results in a different flow and performance behavior as compared to the full-length plug nozzle. At lower pressure ratios an open wake flow establishes, with a pressure level practically equal to the ambient pressure (Fig. 17, right column, top). At a certain pressure ratio close to the design pressure ratio of the full-length plug nozzle, the base flow suddenly changes its character and turns over to the closed form, characterized by a constant base pressure that is no longer influenced by the ambient pressure. Analyses indicate that shorter plug bodies with higher truncations trigger an earlier change in wake flow at pressure ratios below the design pressure ratio. At the transition point the pressure within the wake approaches a value that is below ambient pressure, and the full base area induces a negative thrust (Fig. 17, right column, center). This thrust loss depends on the percentage of truncation and the total size of the base area. Published experimental data and numerical simulations reveal an increasing thrust loss for shorter plug bodies, because the total base area increases.

Beyond the transition point, the pressure within the closed wake remains constant. At these lower ambient pressures, the base pressure is then higher than the ambient pressure, resulting in a positive thrust contribution of the total base area. Performance data of a numerically simulated truncated plug nozzle are shown in Fig. 19, and compared to the same plug nozzle with full-length central body and a conventional bell nozzle. Design parameters for this truncated plug nozzle are the same as for the full length plug (see Fig. 18 and Table 2).

Figure 20 shows a typical photograph of a sea-level hot-run test with a truncated, toroidal subscale plug nozzle, performed at DLR.[5] Nozzle design data are included in Table 2. For comparison of experimental results with numerical computations, the flowfield of the toroidal plug nozzle was calculated with a numerical method,[10] and Fig. 20 shows the calculated Mach-number distribution in the combustion chamber and nozzle. Principal physical processes like expansion waves, shocks, and the recirculating base-flow region are in good agreement. Both the experiment and the numerical simulation show that the flow separates from the conical plug body before reaching its truncated end. Recent results on experiments with plug nozzles published in Ref. 28 also reveal separation of the flow from the central plug body for conical contours. In contrast, no separation was observed for contoured central plug bodies designed with the method proposed in Ref. 29. Recent numerical simulations of contoured plug nozzles performed at DLR within the ESA Advanced Rocket Propulsion Technology (ARPT) Program on advanced rocket propulsion also show that no flow separation occurs from well-contoured, full-length central plug bodies.[26] Principal flowfield developments predicted by these numerical simulations are again in a good agreement with experimental data published in Ref. 28. Within the frame of this ESA ARPT Program performance and flow behavior of clustered plug nozzles at different truncations are being examined by European industries [Société Européenne de Propulsion (SEP), Volvo, Dasa] and research institutes (ONERA, DLR) with subscale cold-flow plug models[26] (Table 3). Numerous experimental investigations on subscale models of circular and clustered plug nozzles with cold- and hot-gas flow were performed at the Keldysh Center with and without external flows. Thrust characteristics, pressure and heat-flux distributions along the plug, and acoustic characteristics of the circular jet were investigated.

2. *Linear Plug Nozzles*

Performance behavior and flowfield development for linear plug nozzles as a function of ambient pressures are in principle similar to those of circular plug nozzles (Fig. 17). However, special attention must be paid to the influence of both end sides, where the surrounding flow disturbs the expanding flowfield, resulting in an expansion of the flow normal to the main flow direction and, therefore, in an effective performance loss.

Table 3 Design parameters for linear and toroidal subscale plug nozzles[a]

Design data	Linear plug (FESTIP)	Circular, clustered plug (ARPT)
Chamber pressure p_c	8.75 bar	8.0 bar
Driving gas	Air	Air
Mass flow rate $\dot{m}$	5.95 kg/s	5.46 kg/s
Design pressure ratio p_c/p_{amb}	200	200
Geometric area ratio ε	12.65	12.65

[a]Used in the ESA FESTIP and ESA ARPT studies.

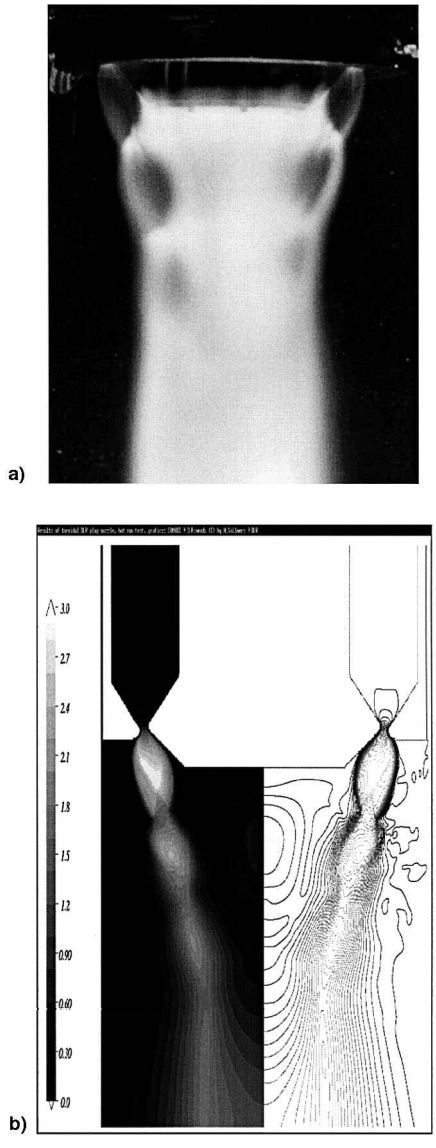

Fig. 20 Plug nozzle flowfield, experiment vs numerical simulation: a) toroidal plug nozzle experiment with gas-oil/nitric-acid propellant combination, side view photograph, and b) computational results of toroidal plug nozzle, Mach number distribution, full gray and isolines, centerline section.

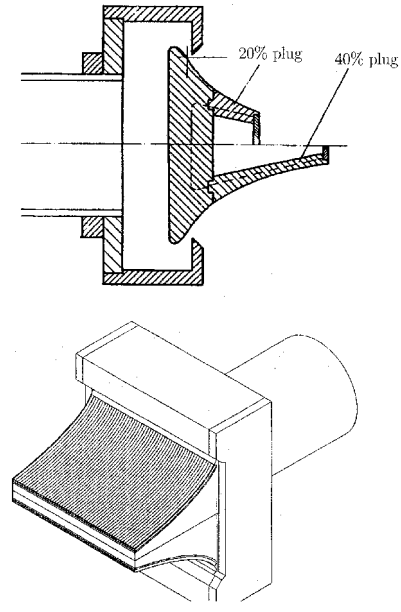

Fig. 21 Design of linear subscale plug nozzle of the ESA FESTIP Technology Program (plug size: 192 mm high, 214 mm wide).

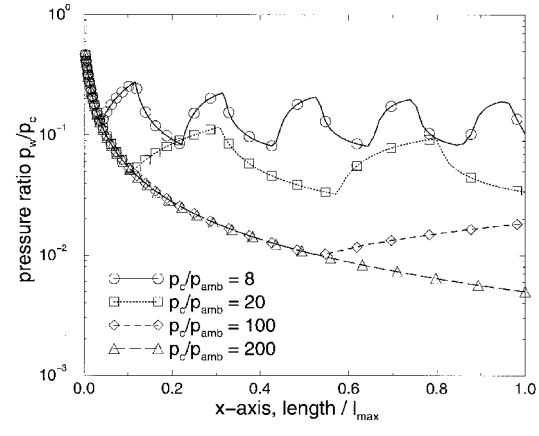

Fig. 22 Calculated wall pressure data for linear subscale plug nozzle at different pressure ratios.

The change of wake flow behavior may be strongly influenced by the penetration of ambient pressures through both end sides, particularly for truncated plug nozzles. End plates, as foreseen for the linear plug nozzle of the X-33 demonstrator vehicle, could be used to avoid this ambient pressure penetration.

Within the framework of the ESA FESTIP Technology Program "Technology Developments on Rocket and Air Breathing Propulsion for Reusable Launch Vehicles," subscale cold-gas tests and numerical simulations of linear plug nozzles are being performed by Dasa at the high-speed wind tunnel [Hochgeschwindigheitswind kanal (HWK) in Bad Salzungen, Germany] of the Technical University of Dresden.[7,19] Design parameters for the linear plug model are included in Table 3. Figure 21 shows the baseline model with a linear throat. After passing the linear throat the flow expands directly onto the plug surface. A second model will be tested with a bell-shaped linear nozzle extension following the linear throat for internal expansion prior to further external expansion onto the plug surface.[19] The contour of the plug was designed by the method of Angelino,[29] and three different plug lengths as 5, 20, and 40% of the ideal length were tested. Figure 22 shows calculated wall pressures for the full-length plug for different ambient pressures, simulating the operational range of sea-level operation up to higher-altitude operation. The flow structure in form of the left- and right-running characteristics at two pressure ratios is shown in Fig. 23. For lower pressure ratios than the design pressure ratio of $p_c/p_{amb} = 200$, the influence of the

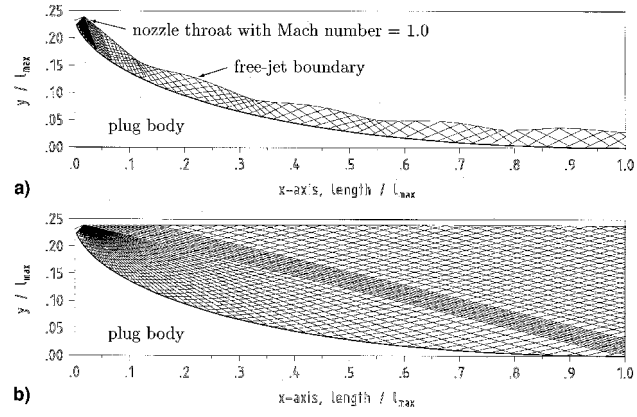

Fig. 23 Left- and right-running characteristics in flowfield at two pressure ratios, p_c/p_{amb}, = a) 8 and b) 200 (inviscid analysis with method of characteristics).

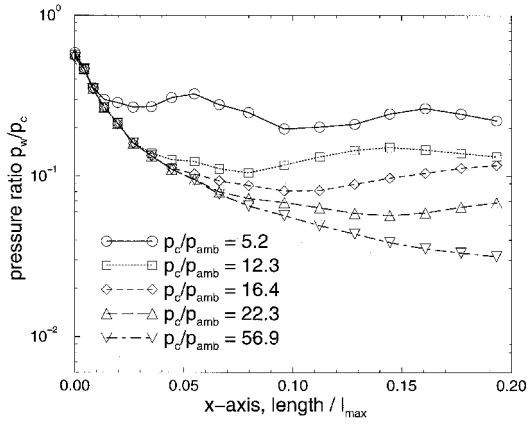

Fig. 24 Measured wall pressure data of linear subscale plug nozzle at different pressure ratios and truncations, 20% plug body.

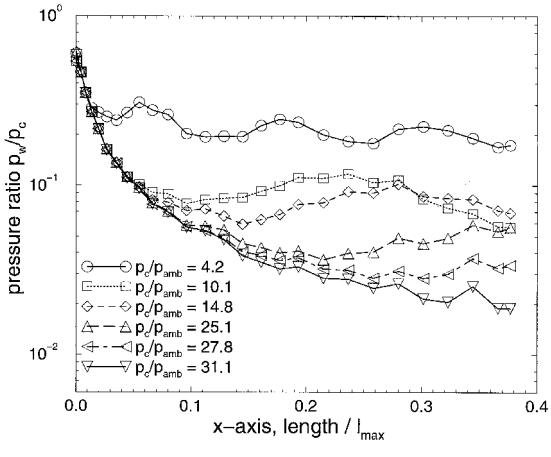

Fig. 25 Measured wall pressure data of linear subscale plug nozzle at different pressure ratios and truncations, 40% plug body.

system of recompression shocks and expansion waves on the wall pressure distribution (Figs. 17 and 22), can be seen by the waviness of the pressure distribution on the plug surface. First experimental results are shown in Figs. 24 and 25, which also show the waviness of the pressure distribution for low-pressure ratios.

3. Plug Nozzles, Final Aspects

The performance of circular and linear plug nozzles is adversely affected by the external airstream flow, i.e., the aspiration effect of the external flow slightly reduces performance and favors an earlier change in wake-flow development for truncated plug nozzles.[32–35] Cold-flow tests showed that the effect of external flow on performance is confined to a narrow range of external flow speeds with Mach numbers near unity.

The altitude compensation capability of circular and linear plug nozzles for higher ambient pressures is indisputable. Because plug nozzles lose this capability for pressure ratios above the design pressure ratio, the latter should be chosen as high as possible. Taking this into account, plug nozzles will feature an even better overall performance than those shown in Figs. 18 and 19. Unfortunately, for equal geometrical area ratios, plug nozzles perform worse at high altitude than do conventional bell nozzles because of truncation and clustering. For high-area-ratio nozzles with relatively short lengths, plug nozzles perform better than conventional bell nozzles. In addition to having excellent capabilities for altitude compensation, plug nozzles have additional advantages, including ease in vehicle and engine integration.

C. E–D Nozzles

An expansion–deflection (E–D) nozzle is shown in Fig. 26. E–D nozzles were at one time thought to have capabilities for altitude compensation because the gas expansion takes place with a constant pressure free boundary. Thus, the aerodynamic behavior of E–D nozzles as a function of altitude is in principle quite similar to plug nozzles, because the expansion process is controlled by the ambient pressure; hence, by the altitude. In contrast to plug nozzles, however, the expansion process is controlled from inside the nozzle for E–D nozzles. At low altitude, the higher ambient pressure limits the gas expansion, resulting in a low effective expansion area ratio. The exhaust gas is adapted to the ambient pressure level by

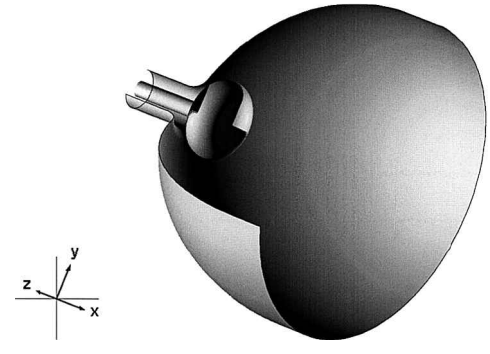

Fig. 26 Sketch of an E–D nozzle.

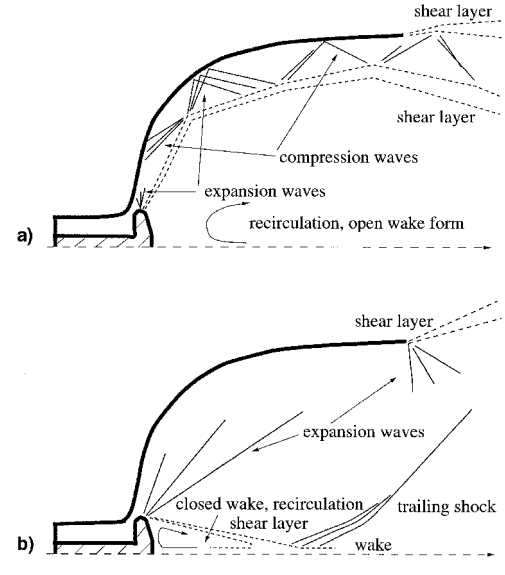

Fig. 27 Flow phenomena of an E–D nozzle, with a) open and b) closed wakes.

systems of recompression and expansion waves (Fig. 27). At higher altitude, the lower ambient pressure allows more gas expansion within the nozzle, resulting in a higher effective expansion area ratio. But in contrast to plug nozzles, the pressure in the wake of the center plug is always less than the ambient pressure because of the aspiration effect. This occurs at low pressure ratios when the wake is opened and results in an aspiration loss. Furthermore, because the exhaust flow expands to this base pressure rather than to the ambient pressure level, wall pressures downstream are overexpanded. This results in an additional overexpansion loss. As the pressure ratio increases, the wake region closes and is thus totally isolated from the ambient environment (see Fig. 27). The behavior during transition from open wake to closed wake is again equal to plug nozzles, and the base pressure in the closed-wake region is essentially independent of the ambient pressure.

The E–D nozzle concept has also been a subject of numerous analytical and experimental studies. Results from these studies show that E–D nozzle capabilities for altitude compensation are poor, and are in fact worse than those of plug nozzles, because of aspiration and overexpansion losses.[35] For high-area-ratio nozzles with a relatively short length, an E–D nozzle performs better than a comparable conventional bell nozzle at the same length because of lower divergence and profile losses than the bell nozzle.

The advantages of the E–D nozzle concept include its small engine envelope and no moving parts. However, like toroidal plug nozzles, E–D nozzles have the disadvantage of having higher throat heat fluxes relative to a conventional bell nozzle with an equal throat area. The higher throat heat flux results again from the relatively thin annular throat gap. This problem, however, can be remedied with the modular thrust cell cluster concept. Additional advantages of E–D nozzles with clustered thrust cells are the same as those already discussed for the clustered plug nozzle concept, with regard to ease in manufacturing, thrust vector control by throttling or shutting off an individual or group of thrust cells, and lower nozzle throat heating.

D. Nozzles with Throat Area Varied by a Mechanical Pintle

This nozzle concept utilizes a conventional bell nozzle with a fixed exit area and a mechanical pintle in the combustion chamber and throat region to vary the throat area and, hence, the expansion area ratio. The area of the nozzle throat—an annulus between the pintle and the shroud—is varied by moving the pintle axially.

The pintle concept has been used in solid rocket motors as a mean to provide variable thrust. The concept, in principle, allows a continuous variation of the throat area and, thus, optimum expansion area ratios throughout a mission. However, it requires an actuator and a sophisticated control system. The concept raises issues of engine weight, design complexity, cooling of the pintle and nozzle throat, and reliability.

In Ref. 36, the aerodynamic performances of nozzles with five different pintle geometries were calculated and compared with a reference bell nozzle. The performance losses of these pintle nozzles when compared with the bell nozzle are in the range of 1–2.5%. Performances of a fixed pintle geometry at three different locations were also calculated. The results show that the performance loss varies with the pintle location.

E. Dual-Mode Nozzles

Dual-mode rocket engines using one or two fuels offer a trajectory-adapted dual-mode operation during the ascent of a launcher, which may be of significant advantage for single-stage Earth-to-orbit vehicles as compared to conventional rocket engines with bell-type nozzles. This engine concept involves the use of a dense propellant combination with moderate performance during liftoff to provide high thrust during the initial flight phase, and a better performing propellant combination in vacuum, which result in higher specific impulse. The fuels are burned in two different combustion chambers, with one located completely inside the other in the case of engines with dual-throat nozzles, or with a conventional bell thrust chamber surrounded by an annular thrust chamber in the case of dual-expander engines. This type of engine has a built-in acceleration–reduction capability, achieved by shutting down one of two thrust chambers. The total engine thrust is then provided by the remaining thrust chamber with the use of the total nozzle exit area leading to an increase in specific impulse. Apart from the indicated benefits of dual-mode engines, which will be discussed in more detail later, their de-

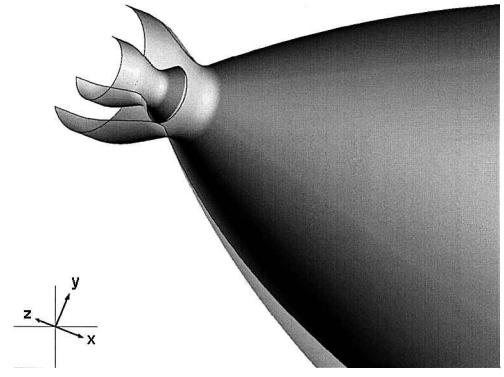

Fig. 28 Sketch of a dual-throat nozzle, view of combustion chamber and throat region.

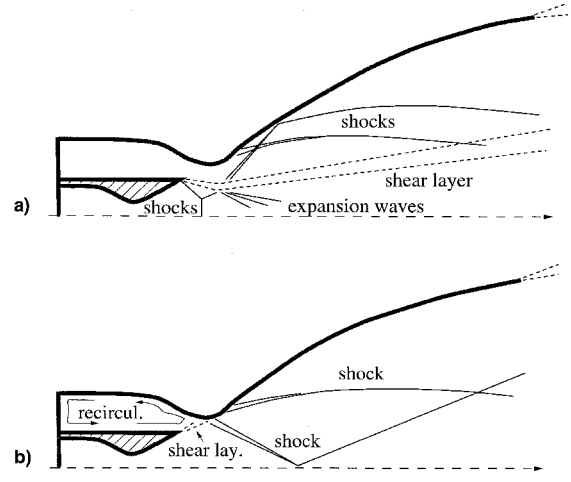

Fig. 29 Flow phenomena during a) sea-level and b) high-altitude operations.

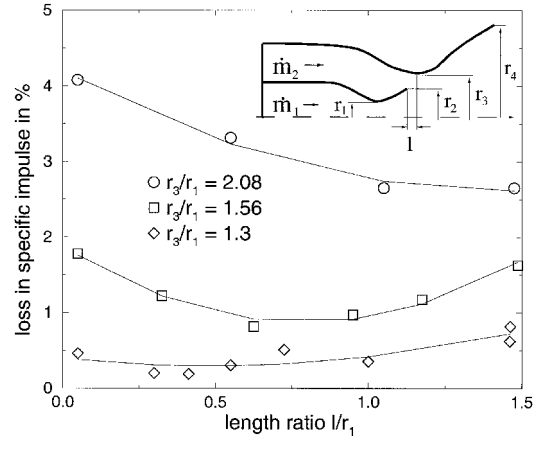

Fig. 30 Performance losses in dual-throat nozzles as a function of nozzle design parameters (with $r_4/r_1 = 3.52$, $r_2/r_1 = 1.16$, and $\dot{m}_2 = 0.0$).

velopment and construction require considerable technological effort.

1. Dual-Throat Nozzles

A dual-throat nozzle configuration is shown in Fig. 28. It consists of two conventional bell-thrust chambers, with one located completely inside the other. At low altitude, the outer thrust chamber operates with the inner thrust chamber running in parallel. In this operation mode the engine has a larger throat providing a moderate expansion area ratio. During the mission, the outer thrust chamber is shut off and operation continues with only the inner engine. In this configuration, flow from the inner engine expands and attaches supersonically to the outer engine, resulting in a higher expansion area ratio for the remainder of the burn. Flow phenomena in both operation modes are included in Fig. 29.

Hot-fired tests at Aerojet were conducted to provide heat transfer data that were very useful for the thermal analysis and design of the dual-throat nozzle configuration.[37] These tests showed that flow separation occurred in the inner engine nozzle at higher ratios of outer to inner chamber pressures during the first operation mode with both chambers burning in parallel. The flow separation resulted in a higher heat load to the inner nozzle. Subscale tests performed at the Keldysh Center[3] have shown that the additional loss caused by the nozzle contour discontinuity during vacuum operation with active inner chamber is in the range of 0.8–4%, depending on geometrical data (see Fig. 30). This high-performance loss results from the interaction of the inner chamber jet with the outer chamber nozzle wall.[3] The decrease of the jet incidence angle on the wall by means of gas injection through the outer chamber reduces this performance loss by 0.4–0.7%.[3]

2. Dual-Expander Nozzles

A dual-expander nozzle has two concentric thrust chambers and nozzles. It consists of a conventional bell thrust chamber surrounded by an annular thrust chamber. Both chambers have short primary nozzles, which end in a common divergent nozzle extension. Figure 31 shows a typical dual-expander nozzle configuration. At low altitude, both thrust chambers operate, sharing the same exit area, which results in a moderate expansion area ratio. Part way into the mission, one thrust chamber is shut off, allowing the other nozzle to use the whole exit area, creating a high-expansion-area ratio for the remainder of the burn. In principle, the two operation modes are comparable to those of dual-throat nozzles.

Numerical simulations of the flowfields in dual-expander nozzles during all operation modes have been performed at Aerojet,[38] DLR,[39] and the Keldysh Center. Aerojet simulations are based on an engine design using different propellants, hydrocarbon/oxygen for the inner chamber and hydrogen/oxygen for the outer chamber, whereas DLR simulations are based on a combined vehicle/engine analysis using single-fuel/single-mixture ratio dual-expander engines with hydrogen/oxygen. Table 4 summarizes combustion chamber parameters. Flow phenomena observed in numerical simulations are shown in Fig. 32a for the mode 1 operation with both thrust chambers burning. Compression waves are induced near the inner nozzle lip as a result of the strongly inhomogeneous flow character at the point where both exhaust gases of inner and outer combustion chamber merge into the common divergent nozzle part. Up and down variations of pressure ratios at the lip did not change this wave formation, even in cases of significantly lower exit pressures in the inner nozzle compared to the pressure field of the outer nozzle at the lip. Further downstream the compression waves interact with the wall, resulting in a reflection of the compression waves back into the flowfield.

During mode 2 operation a strong expansion of the outer nozzle flow is observed, when the expansion ratio suddenly increases at the end of the nozzle lip. The flow is directed toward the axis of symmetry. Near the centerline the flow then turns over to the axial direction, inducing a recompression shock. The static pressure rises significantly in this recompression region on the centerline. A sub- and supersonic recirculation zone establishes in the inner chamber of the dual-expander nozzle. Figure 32b emphasizes the essential flow pattern in this operation mode.

These analyses have shown that dual-expander nozzles produce high performance in both operation modes.[38,39] Figure 33 summarizes performance behavior as a function of flight altitude for the dual-expander engine simulated at DLR. For comparison, performance data are included for two reference bell

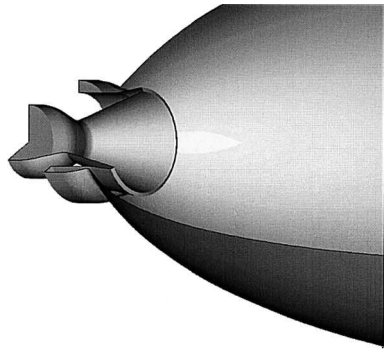

Fig. 31 Sketch of a dual-expander nozzle, view of combustion chamber and throat region.

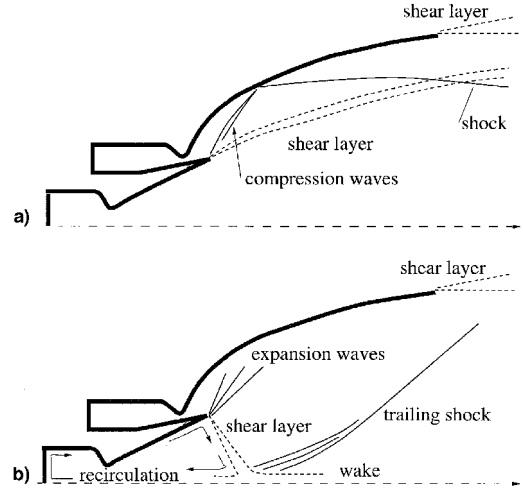

Fig. 32 Flow phenomena in a dual-expander nozzle during a) sea-level- and b) high-altitude operation.

Table 4 Thrust chamber parameters for simulated dual-expander nozzles[a]

	Aerojet		DLR	
Operation mode	First (in/out)	Second (in/out)	First (in/out)	Second (in/out)
Propellants	C_3H_8–O_2/H_2–O_2	—/H_2–O_2	H_2–O_2/H_2–O_2	—/H_2–O_2
Chamber pressure p_c	414/207 bar	—/207 bar	200/200 bar	—/200 bar
Mixture ratio $\bar{r}$	3.3/7	—/7	7/7	—/7
Exit area ratio ε	69	146	58	116

[a]Inner/outer chambers.

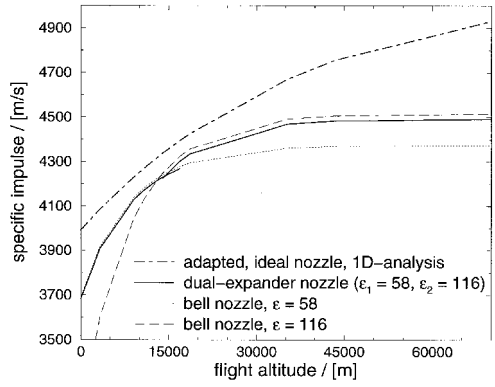

Fig. 33 Performance data for a dual-expander nozzle.

nozzles that have the same area ratios as the dual-expander nozzle during its two operation modes. Losses because of the nonhomogeneous exit flow and the induced shocks are comparable with corresponding values of both conventional nozzles.[1]

Within the design process of dual-expander engines it is necessary to take into account that the nonburning chamber is exposed to high heat fluxes and pressure oscillations during mode 2 operation, which might reach a high level and lead to structural disintegration of the inner nozzle structure. Therefore a mode-2 operation with bleed gas generation at a rather low thrust chamber pressure level in the inner chamber seems to be advantageous. Because of the bleed gas generation in the primary chamber, the overall mass flow rate during this alternative mode-2 operation is increased. In addition, the reduction of the effective exit area ratio results in minor impulse degradations during this operation mode when compared with the mode-2 operation with no bleed gas generation.

Several analytical works on SSTO- and two-stage-to-orbit (TSTO)-vehicles using hydrogen/propane or hydrogen/methane as fuels revealed the lowest vehicle dry masses for dual-mode engines in comparison to other engines.[14,39] Other dual-mode engines using hydrogen as the single fuel but using two mixture ratios also revealed some benefits over conventional engines for SSTO- and TSTO applications. Even a single-fuel operation with constant mixture ratios in both combustion chambers indicated a gain in launcher performance.[40]

V. Conclusions

Several nozzle concepts that promise gains in performance over conventional nozzles were discussed in this paper, including performance enhancements achieved by slight modifications of existing nozzles, e.g., through cool gas injection into the supersonic nozzle part. It is shown that significant performance gains result from the adaptation of the exhaust flow to the ambient pressure, and special emphasis was given to altitude adaptive nozzle concepts.

A number of nozzle concepts with altitude-compensating capability were identified and described. To assist the selection of the best nozzle concept for launch vehicle applications, the performance of the nozzles must be characterized. This can be done using computational fluid dynamics (CFD) and/or cold-flow tests. Existing CFD methods that are in use in the aerospace industry and at research institutes have been verified for a wide number of sub- and full-scale experiments, and provide sufficiently reliable performance determination for the different nozzle types.

Theoretical evaluations, numerical simulations, and test results showed that the different concepts have real altitude-compensating capabilities. However, the compensation capabilities are limited and there are some drawbacks associated with each of the concepts. Additional performance losses are induced in practically all of these nozzle concepts when compared to an ideal expansion, mainly because of the nonisentropic effects such as shock waves and pressure losses in recirculation zones. However, these additional performance losses are less than 1–3%, depending on the different nozzle concepts.

Four nozzle concepts have been selected for further evaluation under a NASA/Aerojet cooperative agreement. They include a plug nozzle, an E–D nozzle, a dual-bell nozzle, and a dual-expander nozzle. The nozzles, in addition to a reference bell nozzle, have been designed by Aerojet for cold flow tests. CFD calculations performed at Aerojet demonstrated that all of these nozzles have high and approximately equal performances at the design points.

In Europe special attention is being paid to plug- and dual-bell nozzles. Different plug nozzle concepts are being tested in cold-flow tests within the ESA ARPT (clustered plug nozzle) and ESA FESTIP (linear plug nozzle) contracts. In addition to experiments, three-dimensional numerical simulations on these nozzle concepts are being performed. Additional experiments on different nozzle concepts with forced-flow separation devices, e.g., dual-bell nozzles, are currently planned at DLR.

Different advanced nozzle concepts have been examined and are under examination now at the Keldysh Center with both CFD calculations and experiments on the Nozzle Differential Facility, which has a nozzle performance determination error of about 0.05%. This high accuracy is achieved by simultaneously running the test nozzle and a reference nozzle, both mounted on a common longitudinal axis. The performance characteristics of the reference nozzle are well known, and the thrust difference is measured with strain gauges. This facility is equipped with a wind tunnel to determine nozzle thrust performance in the presence of external transonic flows with Mach numbers up to 1.2.

In addition to aerodynamic performance, other technical issues (weight, cost, design, thermal management, manufacturing, system performance, and reliability) must be addressed. Furthermore, before a final decision can be made as to which nozzle concept offers the greatest benefits with regard to an effective payload mass injection, combined launcher and trajectory calculations must be performed and compared to a reference launcher concept with conventional nozzles. Different nozzle efficiencies, which account for the additional losses of advanced rocket nozzles and are extracted from numerical simulations and experiments, must be taken into account.

At least for some of these nozzle concepts, the plug nozzle, the dual-bell nozzle, and the dual-expander nozzle, benefits with regard to lower overall launcher masses have been demonstrated in the literature. Furthermore, the plug nozzle concept will be the first in flight of all of these advanced nozzle concepts, with the X-33 demonstrator vehicle.

Acknowledgment

Presented as Paper 1.8 at the 3rd International Symposium on Space Propulsion, Beijing, People's Republic of China, Aug. 11–13, 1997.

References

[1]Manski, D., and Hagemann, G., "Influence of Rocket Design Parameters on Engine Nozzle Efficiencies," *Journal of Propulsion and Power*, Vol. 12, No. 1, 1996, pp. 41–47.

[2]"Liquid Rocket Engine Nozzles," *NASA Space Vehicle Design Criteria*, NASA SP-8120, 1976.

[3]Dumnov, G. E., Nikulin, G. Z., and Ponomaryov, N. B., "Investigation of Advanced Nozzles for Rocket Engines," *Space Rocket Engines and Power Plants*, Vol. 4, No. 142, NIITP, 1993, pp. 10.12–10.18 (in Russian).

[4]Nguyen, T. V., and Pieper, J. L., "Nozzle Flow Separation," *Proceedings of the 5th International Symposium of Propulsion in Space Transportation* (Paris, France), 1996.

[5]Manski, D., "Clustered Plug Nozzles for Future European Reusable Rocket Launchers," German Aerospace Research Establishment, 643-81/7, Lampoldshausen, Germany, 1981 (in German).

[6]Horn, M., and Fisher, S., "Dual-Bell Altitude Compensating Noz-

zles," NASA CR-194719, 1994.
[7]Immich, H., and Caporicci, M., "FESTIP Technology Developments in Liquid Rocket Propulsion for Reusable Launch Vehicles," AIAA Paper 96-3113, July 1996.
[8]Summerfield, M., Foster, C., and Swan, W., "Flow Separation in Overexpanded Supersonic Exhaust Nozzles," *Jet Propulsion*, Sept. 1954, pp. 319–321.
[9]Schmucker, R., "Flow Processes in Overexpanding Nozzles of Chemical Rocket Engines," Technical Univ., TB-7,-10,-14, Munich, Germany, 1973 (in German).
[10]Hagemann, G., Schley, C.-A., Odintsov, E., and Sobatchkine, A., "Nozzle Flowfield Analysis with Particular Regard to 3D-Plug-Cluster Configurations," AIAA Paper 96-2954, July 1996.
[11]Dumnov, G. E., "Unsteady Side-Loads Acting on the Nozzle with Developed Separation Zone," AIAA Paper 96-3220, July 1996.
[12]Nave, L. H., and Coffey, G. A., "Sea-Level Side-Loads in High Area Ratio Rocket Engines," AIAA Paper 73-1284, July 1973.
[13]Pekkari, L. O., "Advanced Nozzles," *Proceedings of the 5th International Symposium of Propulsion in Space Transportation* (Paris, France), 1996, pp. 10.4–10.11.
[14]Manski, D., Goertz, C., Saßnick, H.-D., Hulka, J. R., Goracke, B. D., and Levack, D. J. H., "Cycles for Earth-to-Orbit Propulsion," *Journal of Propulsion and Power*, Vol. 14, No. 5, 1998, pp. 588–604.
[15]Hagemann, G., Krülle, G., and Hannemann, K., "Numerical Flowfield Analysis of the Next Generation Vulcain Nozzle," *Journal of Propulsion and Power*, Vol. 12, No. 4, 1996, pp. 655–661.
[16]Voinow, A. L., and Melnikov, D. A., "Performance of Rocket Engine Nozzles with Slot Injection," AIAA Paper 96-3218, July 1996.
[17]Forster, C., and Cowles, F., "Experimental Study of Gas Flow Separation in Overexpanded Exhaust Nozzles for Rocket Motors," Jet Propulsion Lab., Progress Rept. 4-103, California Inst. of Technology, Pasadena, PA, May 1949.
[18]Hagemann, G., and Frey, M., "A Critical Assessment of Dual-Bell Nozzles," AIAA Paper 97-3299, July 1997.
[19]Immich, H., and Caporicci, M., "Status of the FESTIP Rocket Propulsion Technology Program," AIAA Paper 97-3311, July 1997.
[20]Luke, G., "Use of Nozzle Trip Rings to Reduce Nozzle Separation Side Force During Staging," AIAA Paper 92-3617, July 1992.
[21]Chiou, J., and Hung, R., "A Study of Forced Flow Separation in Rocket Nozzle," Alabama Univ., Final Rept., Huntsville, AL, July 1974.
[22]Schmucker, R., "A Procedure for Calculation of Boundary Layer Trip Protuberances in Overexpanded Rocket Nozzles," NASA TM X-64843, 1973.
[23]Goncharov, N., Orlov, V., Rachuk, V., Shostak, A., and Starke, R., "Reusable Launch Vehicle Propulsion Based on the RD-0120 Engine," AIAA Paper 95-3003, April 1995.
[24]Clayton, R., and Back, L., "Thrust Improvement with Ablative Insert Nozzle Extension," *Jet Propulsion*, Vol. 2, No. 1, 1986, pp. 91–93.
[25]Parsley, R. C., and van Stelle, K. J., "Altitude Compensating Nozzle Evaluation," AIAA Paper 92-3456, July 1992.
[26]"ARPT—Advanced Rocket Propulsion Technology Program, Final Reports Phase 1 and 2," European Space Agency—European Space Research and Technology Centre, The Netherlands, 1996.
[27]Rommel, T., Hagemann, G., Schley, C.-A., Manski, D., and Krülle, G., "Plug Nozzle Flowfield Calculations for SSTO Applications," *Journal of Propulsion and Power*, Vol. 13, No. 6, 1997, pp. 629–634.
[28]Tomita, T., Tamura, H., and Takahashi, M., "An Experimental Evaluation of Plug Nozzle Flow Field," AIAA Paper 96-2632, July 1996.
[29]Angelino, G., "Theoretical and Experimental Investigations of the Design and Performance of a Plug Type Nozzle," NASA TN-12, July 1963.
[30]Lee, C. C., "Fortran Programs for Plug Nozzle Design," NASA TN R-41, March 1963.
[31]Nguyen, T. V., Spencer, R. G., and Siebenhaar, A., "Aerodynamic Performance of a Round-to-Square Nozzle," *Proceedings of the 35th Heat Transfer and Fluid Mechanics Institute*, 1997.
[32]Beheim, M. A., and Boksenbom, A. S., "Variable Geometry Requirements in Inlets and Exhaust Nozzles for High Mach Number Applications," NASA TM X-52447, 1968.
[33]Valerino, A. S., Zappa, R. F., and Abdalla, K. L., "Effects of External Stream on the Performance of Isentropic Plug-Type Nozzles at Mach Numbers of 2.0, 1.8 and 1.5," NASA 2-17-59E, 1969.
[34]Mercer, C. E., and Salters, L. E., Jr., "Performance of a Plug Nozzle Having a Concave Central Base with and Without Terminal Fairings at Transonic Speeds," NASA TN D-1804, May 1963.
[35]Wasko, R. A., "Performance of Annular Plug and Expansion-Deflection Nozzles Including External Flow Effects at Transonic Mach Numbers," NASA TN D-4462, April 1968.
[36]Smith-Kent, R., Loh, H., and Chwalowski, P., "Analytical Contouring of Pintle Nozzle Exit Cone Using Computational Fluid Dynamics," AIAA Paper 95-2877, 1995.
[37]Ewen, R. L., and O'Brian, C. J., "Dual-Throat Thruster Results," AIAA Paper 86-1518, 1986.
[38]Nguyen, T. V., Hyde, J. C., and Ostrander, M. J., "Aerodynamic Performance Analysis of Dual-Fuel/Dual-Expander Nozzles," AIAA Paper 88-2818, 1988.
[39]Hagemann, G., Krülle, G., and Manski, D., "Dual-Expander Engine Flowfield Simulations," AIAA Paper 95-3135, July 1995.
[40]Manski, D., Hagemann, G., and Saßnick, H. D., "Optimization of Dual-Expander Rocket Engines in Single-Stage-to-Orbit Vehicles," *Acta Astronautica*, Vol. 40, No. 2–8, 1997, pp. 151–163.